



## TiO<sub>2</sub>/Ti thin-film electrode manufacturing equipment and combined external circuit photoelectrical catalytic process for reducing silver ions

Chao-Lang Kao<sup>a,b,\*</sup>, Yung-Hsu Hsieh<sup>a</sup>, Ming-Yi Chang<sup>a</sup>, Chia-Hsin Li<sup>a</sup>, Chin-Chuan Liu<sup>a</sup>

<sup>a</sup> Department of Environmental Engineering, National Chung Hsing University, 250, Kuo Kuang Road, Taichung 402, Taiwan

<sup>b</sup> Department of Chemical and Materials Engineering, National Chin Yi University of Technology, 35, Lane 215, Sec. 1, Chung-Shan Road, Taiping, Taichung 411, Taiwan

### ARTICLE INFO

#### Article history:

Received 4 January 2008

Received in revised form 17 June 2008

Accepted 18 June 2008

#### Keywords:

External circuit

Photoelectrocatalytic

TiO<sub>2</sub>/Ti

Photoanodes

Silver recovery

### ABSTRACT

In this study, a nano-class TiO<sub>2</sub>/Ti thin-film electrode was made using the atmospheric pressure chemical vapor deposition (APCVD). The electrode was combined with an external circuit and anode bias to study the efficiencies of silver ions reduction and acetic acid decomposition. Results of SEM images and XRD patterns of the TiO<sub>2</sub>/Ti thin-film electrode surface show that the thin-film electrode made using the APCVD method can be as size as 30 nm with the TiO<sub>2</sub> photoelectric catalyst in anatase crystal form. More obvious agglomeration of TiO<sub>2</sub> particles was observed for shorter APCVD sprayed times. Results of the light response study show that the electrode has a rapid response time to 365 nm UV light to produce electricity with 7 μA/cm<sup>2</sup> density. Additionally, results of the photocatalytic studies using the electrode combined with an external circuit in the photoelectrical catalytic studies to reduce silver ions reveal that with a reaction time of 180 min, the photocatalytic process will reduce 70% of silver ions in high-concentrated solution (1000 mg/l as Ag) and 93% silver ions in low-concentrated solution (108 mg/l as Ag). When the irradiation time is extended to 240 min, the silver reduction efficiency is as high as 99.8%. Higher solution pH is favorable to the photoelectrical reduction of silver while the anode bias does not benefit the silver reduction efficiency but favors the decomposition of acetic acid. However, the process decomposes less than 10% of acetic acid. The external circuit will transmit the photo-generated electrons to the cathode surface thus reducing the combination of electron and holes at the anode surface. As the reduction of precious metals is concerned, the external circuit is capable of avoiding the metal deposition at the catalyst surface to cause catalyst poison or light shielding that are known to reduce the photo utilization efficiency.

© 2008 Elsevier B.V. All rights reserved.

### 1. Introduction

Silver is a basic precious metal that has wide uses in electroplating, die casting alloy, coins, silverware, photographic film and chemical manufacturing. With advances in science and technology as well as improved living standards, consumption of precious metal increases tremendously. Data reported by Taiwan Directorate General of Customs reveal that the annual consumption of silver in Taiwan is 160 thousand tons. Thus, recovery and reuse of silver from discarded silver-containing wastes is of great urgency. Silver ions combined with anions (S<sub>2</sub>O<sub>3</sub><sup>2-</sup>, SO<sub>3</sub><sup>2-</sup>, Br<sup>-</sup>, Cl<sup>-</sup>) in water to form complexes; long-term consumption of the water containing silver ions has been considered to cause serious health hazards. In drinking water, the silver concentration is limited to less than

\* Corresponding author at: Department of Environmental Engineering, National Chung Hsing University, 250, Kuo Kuang Road, Taichung 402, Taiwan.  
Tel.: +886 4 22855367; fax: +886 4 23926617.

E-mail address: [kaocl@mail.nctu.edu.tw](mailto:kaocl@mail.nctu.edu.tw) (C.-L. Kao).

0.05 mg/l while for industrial wastewater discharges, it is limited to 0.5 mg/l. Most wasted silver comes from the discarded photographic fixer, which also contains thiosulfate sodium sulfite, acetic acid, and exposed photographic film, from hospital and commercial darkrooms, printing circuit plate industry as well as the waste discharged by electroplating and electronic metal surface treating industries for processing lead frame. The photographic fixer waste discharged by hospitals, which contains more than 6000 mg/l silver, has been proclaimed by Taiwan Environmental Protection Administration a hazardous industrial waste and needs proper treatment. Although the photographic waste fixer discharge from commercial darkroom contains lower silver ions of 3000 mg/l or above, it must be subject to effective treatment for recovering the silver to avoid wasting precious resources and damaging environment.

The silver recovery methods commonly practiced domestically and internationally include: electro-dialysis reduction [1–4], ion exchange [5], solvent extraction [6,7], bio-adsorption [8], ion flotation [9] and homogenous photo catalytic reduction [10].

In recent years, the technology of producing nano photocatalyst has attended to maturity and widely applied for solving environ-

mental pollution problems. In the application of heterocatalyst system, the oxidation/reduction semi-conductor photocatalyst  $\text{TiO}_2$  is attractive because of many advantages, e.g. chemically stable and non-toxic. Its band gap energy is 3.2 eV that covers the reduction potential of  $\text{Ag}^+/\text{Ag}^0$  (+0.799 eV) and  $\text{Ag}(\text{S}_2\text{O}_3)_2^{3-}/\text{Ag}^0$  (+0.01 eV) to effect photocatalytic reduction of silver ions.

Many researchers have applied suspended  $\text{TiO}_2$  particles to conduct the photocatalytic reduction of silver ions but encountered some problems. When the concentration of suspended  $\text{TiO}_2$  is too high, an ultraviolet shielding effect reduces the light efficiency to reduce the reduction capability of photocatalyst. Additionally, the reduced silver metal is mixed with the suspended  $\text{TiO}_2$  leading to subsequent difficulty in separated silver metal [11–21]. Titanium dioxide fixed on thin film has been applied to recover precious metal from aqueous solution and improve the quality of precious metal (gold, silver and platinum) covered  $\text{TiO}_2$  thin-film. The objective is to increase activities of the catalyst by adding silver in water instead of treating silver-containing wastewater. If not properly handled, this process will produce more silver-containing solution. Although the thin-film photocatalyst with  $\text{TiO}_2$  fixation will alleviate the problem of ultraviolet shielding effect in suspended  $\text{TiO}_2$  system, deposition of the recovered metal on the  $\text{TiO}_2$  thin-film surface will also cause ultraviolet shielding effect to poison the catalyst and difficult in recovering the metal [22–25].

To overcome the problems encountered when using either the suspended  $\text{TiO}_2$  or the  $\text{TiO}_2$  membrane method, the atmospheric pressure chemical vapor deposition (APCVD) is applied to make a  $\text{TiO}_2$  thin-film electrode to be used in the photoelectrocatalytic (PEC) system. An external circuit is used to transmit the electrons generated photoelectrically at the anode to the graphite cathode surface for enhancing the reduction of silver ion into silver metal to achieve recovery, separation and purification of silver. Additionally, to reduce the accumulation of photo-generated holes at  $\text{TiO}_2$  thin-film surface and the recombination of photo-generate electron–hole pairs, a co-existed organic substance (e.g. acetic acid) is used as the hole scavenger thus increasing the efficiency of silver reduction. Finally, anode bias is collocated to assist in improving the photoelectrical efficiency to increase the silver reduction and organic matter decomposition rates.

## 2. Experimental method

### 2.1. Reagents

Tetraisopropyl orthotitanate (TTIP,  $\text{Ti}[\text{OCH}_3(\text{CH}_2)_2]_4$ ), which is the precursor of photocatalyst, was prepared in the lab by mixing silver nitrate ( $\text{AgNO}_3$ , Mallinckrodt, 99%) and Glacial acetic acid ( $\text{CH}_3\text{COOH}$ , J.T. Baker, 99.9%) using deionized water (18.2 m $\Omega$ , Milli-Q).

### 2.2. Preparation of $\text{TiO}_2/\text{Ti}$ thin-film electrode

The  $\text{TiO}_2/\text{Ti}$  thin-film electrode was prepared in the laboratory using the APCVD (atmospheric pressure chemical vapor deposition). After submerged in 9M sulfuric acid for 1 h, the plate substrate was drip washed and then dried. Afterwards, it was placed horizontally in a tubular furnace to be coated by passing nitrogen gas with flow rate controlled at 1:4 to carry the TTIP (Tetraisopropyl orthotitanate) solution, which had been placed in 60 °C water bath, into the 400 °C furnace for 2–6 h. The coated  $\text{TiO}_2/\text{Ti}$  electrode was then removed in a 550 °C furnace to be calcined for 24 h. After cooling down to room temperature, the calcined electrode was cleaned in an ultrasonic washer for 10 min to remove the surface un-fixed

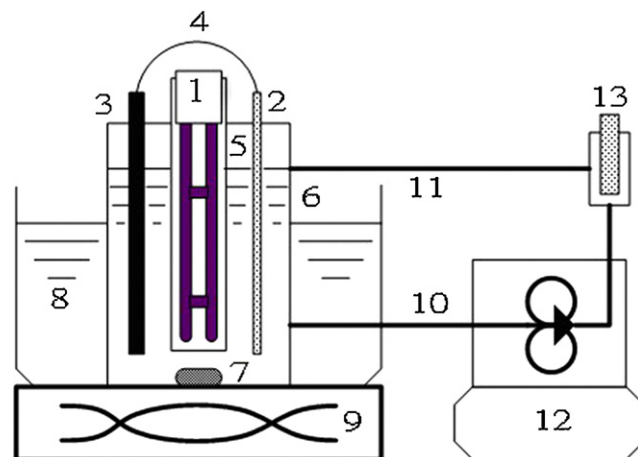


Fig. 1. Schematic diagram showing the reactor setup including: (1) UV lamp; (2) anode ( $\text{TiO}_2/\text{Ti}$  plates); (3) cathode (sticks of graphite); (4) external circuit; (5) quartz tube; (6) outer pyrex cylinder; (7) agitator; (8) circulating water bath; (9) stirrer/hot plates; (10) recycled water outlet; (11) recycled water inlet; (12) peristaltic pump; (13) pH meter.

$\text{TiO}_2$  photocatalyst. It was subsequently dried and preserved in a desiccator for later use.

### 2.3. Photochemical reactor

The 300-ml photochemical reactor was made of a 70-mm i.d. and 150-mm height pyrex container (IWAKI Code 7740 glass, as shown Fig. 1). In the middle, a quartz tube (o.d. 36 mm, i.d. 30 mm) was installed to host UV light (wavelength 365 nm, Sparkei, 13 W/BLB). The reactor was equipped with a magnetic stirrer to mix the content and a peristaltic pump (Cole-Parmer) capable of delivering 300 mg/min liquid. Either side of the reactor was equipped with a  $\text{TiO}_2/\text{Ti}$  thin-film anode and graphite rod cathode. The  $\text{TiO}_2/\text{Ti}$  thin-film electrode reactive area was 5000 mm<sup>2</sup> (25 mm × 100 mm × 2) coated with 0.024 g  $\text{TiO}_2$  resulting in 0.08 g/l solid to liquid ratio and 0.48 mg/cm<sup>2</sup> unit surface area  $\text{TiO}_2$  loading rate. The outside of the reactor was covered with PVC that is impervious to light for eliminating the interference caused by light.

### 2.4. Analytical apparatus

The surface structure of the deposit on the photocatalytic electrode and cathode was analyzed using a scanning electron microscope (SEM, Topcon, ABT-150S) and an X-ray diffractometer (XRD, MAC SIENCE MXP-18).

The light response characteristics and photoelectrical were measured using an electrochemical impedance analyzer (Model 6310, EG&G). The UV intensity was analyzed using a light intensifier meter (I Light, IL 1700).

The soluble silver ion concentration was determined using a flame atomic absorption spectrophotometer (Varian, Spectrr AA 880 Flame); acetic acid concentration was analyzed using an ion chromatography (IC, Metrohm, 790 personal IC). The degree of organic matter mineralization was measured using a Total Organic Carbon (TOC) Analyzer (TOC-VCSN, Shimadzu); pH was determined with a pH meter (IonLab, pH/ion level 2).

## 3. Results and discussion

Fig. 2 shows the surface structure SEM image of  $\text{TiO}_2/\text{Ti}$  thin-film electrode prepared at 6-h APCVD spray time. The  $\text{TiO}_2$  membrane prepared using the APCVD method shows slight agglomeration in

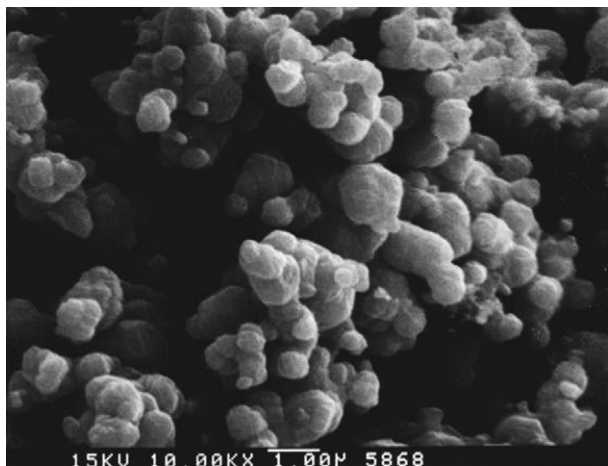


Fig. 2. The SEM images of TiO<sub>2</sub>/Ti thin-film electrodes formed by APCVD at 400 °C, annealed at 550 °C with 6 h sprayed time.

addition to reduced TiO<sub>2</sub> particles size with increasing APCVD spray time. The electrode SEM images shows that after 2-h APCVD spray time, the particles display obvious agglomeration. Since the APCVD spray time is short, when the deposited TiO<sub>2</sub> particles contact the titanium plate that has a larger thermal conductivity coefficient, they are heated up to result in a rapid stacking phenomenon. With increasing APCVD spray time, the TiO<sub>2</sub> thin-film thickness increases. With smaller thermal conductivity coefficient, TiO<sub>2</sub> particles do not show obvious thermal agglomeration. Hence when the APCVD time increases from 2 to 6 h, the dimension of the agglomeration decreases from 6 μm to around 0.5 μm.

The X-ray diffraction patterns of the TiO<sub>2</sub>/Ti thin-film electrode prepared at various APCVD spray times are shown in Fig. 3; obvious peaks are noted to occur at 25.4° and 48.1° (2θ). Compared with the database published by Joint Committee on Powder Diffraction Standards (JCPDS) (Database, JCPDS No. 02-0387), the TiO<sub>2</sub> crystal is identified as anatase with calculated crystal diameter of 30 nm using the Scherrer's formula:

$$d = \frac{\kappa\lambda}{\beta \cos \theta} \tag{1}$$

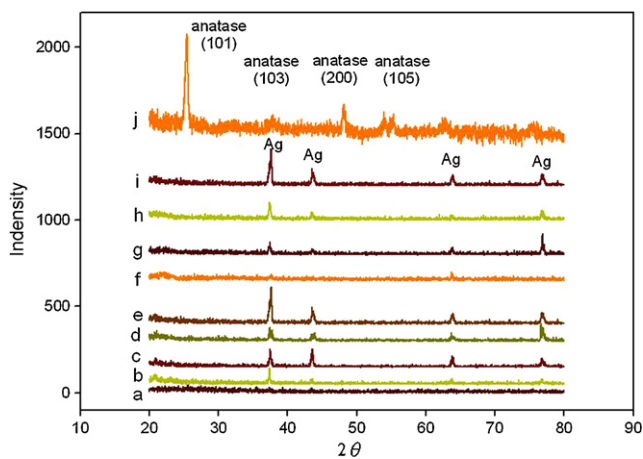


Fig. 3. The XRD pattern (j) of the TiO<sub>2</sub>/Ti thin-film electrodes prepared by APCVD with 6 h sprayed time and the XRD pattern of silver recovered from cathode electrodes at various silver/acetic acid ratios at 3 h reaction time: (a) 1000:1000; (b) 1000:800; (c) 1000:600; (d) 800:1000; (e) 800:800; (f) 800:600; (g) 600:1000; (h) 600:800; (i) 600 mg/l:600 mg/l.

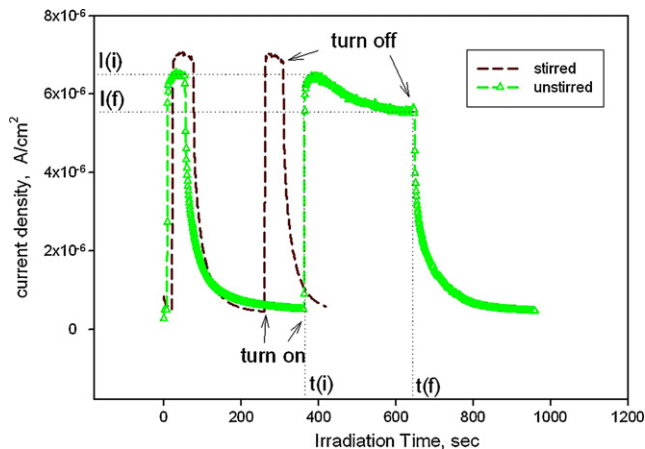


Fig. 4. Transient response of anodic photocurrent density measured in deionized water (experimental conditions: temperature, 25 °C; experiment volume, 300 ml; light intensity, 3 mW cm<sup>-2</sup>; APCVD, 6 h).

where *d* is the crystal size, *β* is the full width at half maximum of an individual peak (FWHM), *κ* is the shape factor of the average crystal, *λ* is the wavelength, and *θ* is the peak position (Bragg angle).

Hence, the APCVD method is confirmed to produce nano-sized TiO<sub>2</sub> membrane.

Using the 365 nm UV light with 3 mW/cm<sup>2</sup> intensity as the light source for conducting the TiO<sub>2</sub>/Ti thin-film electrode light response study, the variation of photocurrent density with respect to irradiation period shown in Fig. 4 indicates that the TiO<sub>2</sub>/Ti thin-film electrode has a rather rapid photo response to UV light. When the UV light is turned on, the photocurrent density rises from 0 to 7 μA/cm<sup>2</sup> within a couple of seconds demonstrating the excellent photo response of the APCVD-produce TiO<sub>2</sub> thin-film electrode with respect to 365-nm UV light. The research results reported by Hagfeldt et al. [26] indicate that the photocurrent instantaneous response kinetic parameter (*D*) will assist in understanding the mechanism of reduced photocurrent. If the “ln(*D*)” term is linearly proportional to irradiation time, the mechanism is recombination of electron–hole pairs; a non-linear relationship reveals that the photocurrent reduction mechanism is rather complicated as depicted by the following function:

$$D = \exp\left(-\frac{t}{\tau}\right) \tag{2}$$

where *D* is defined as  $D = (I(t) - I(f)) / (I(i) - I(f))$ , *τ* is the transient time constant, *I*(*t*) is the anodic or cathodic photocurrent at time *t*, *I*(*i*) the current at *t* = 0, and *I*(*f*) the stationary current. The linear variation of the photocurrent instantaneous response parameter, ln(*D*), versus time reveals that the mechanism for the reduction of photocurrent density at the TiO<sub>2</sub>/Ti thin-film electrode is the competition between the photo generate of electron–hole pairs and their recombination. Results of the experiment on TiO<sub>2</sub> and TiO<sub>2</sub> photocurrent instantaneous response kinetic parameter (ln(*D*)) carried out by Radecka et al. [27] show that a linear variation implying that the photocurrent variation phenomenon can be explained based on the competition between photo generation of electron–hole pairs and recombination of electrons–holes.

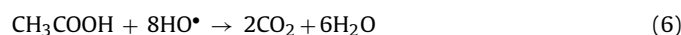
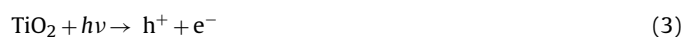
Reactant concentrations are common factors to influence the photocatalytic reactions and systems. In this study, the results of the photocatalytic experiments using the external circuits in carrying out the photocatalytic experiment under various concentrations of silver and acetic acid concentrations. The solution pH values for different set of samples decrease with increasing reaction time because the hole, which has been produced in the photocatalytic

**Table 1**

Relationships between pseudo first-order rate constants, removal efficiencies of silver and acetic acid using the photoelectrocatalytic process at 3 h (experimental conditions: temperature, 25 °C; circulating rate, 300 ml min<sup>-1</sup>; light intensity, 3 mW cm<sup>-2</sup>)

Silver (mg/l)	Acetic acid (mg/l)	Molar ratio	Remained silver (%)	Pseudo first-order rate constants ( $k$ (min <sup>-1</sup> ))	Correlation coefficient ( $R$ )	Remained acetic acid (%)
1000	1000	0.556	30.6	0.0064	0.9920	97.0
1000	800	0.694	59.1	0.0029	0.9957	95.1
1000	600	0.926	45.1	0.0045	0.9980	97.7
800	1000	0.444	26.3	0.0068	0.9877	95.6
800	800	0.556	42.3	0.0055	0.9869	93.2
800	600	0.741	43.4	0.0041	0.9805	98.7
600	1000	0.333	35.0	0.0059	0.9897	99.3
600	800	0.417	21.9	0.0077	0.9817	97.9
600	600	0.556	36.2	0.0047	0.9590	98.5

reaction, oxidizes water into  $\cdot\text{OH}$  and  $\text{H}^+$  (Eqs. (4) and (5)). The hydroxyl radical ( $\cdot\text{OH}$ ) further reacts with acetic acid to produce hydrogen ions ( $\text{H}^+$ ) that consume hydroxyl ions thus causing the solution pH to drop.



As shown in Table 1, different concentration ratios of silver ions to acetic ions lead to the reduction of acetic acid decomposition rate with increasing initial acetic acid concentrations. Overall, the photocatalytic reaction is not effective in decomposing acetic acid with only 5% efficiency under high concentrations of acetic acid. Yang and Tsai [28] reported only 3% acetic acid decomposition rate in 5 h using the photo catalytic system to treat acetic acid. The results obtained by Hidaka et al. [29] on using the photo catalytic decomposition of acetic acid show that the reduction of acetic acid concentration is accompanied by lowering photo-generated current that illustrates the poor acetic acid decomposition efficiency in the photo catalytic process.

The results shown in Fig. 5 on the reduction of silver ion reveal that the efficiency of silver reduction increases with higher initial silver ion concentrations (e.g. 600, 800 and 1000 mg/l) to reach 55–70% in 3 h. The reduction of silver ion reduction is caused by the combination of soluble silver ions with the electrons that has been produced by the production of electron–holes under the irradiation

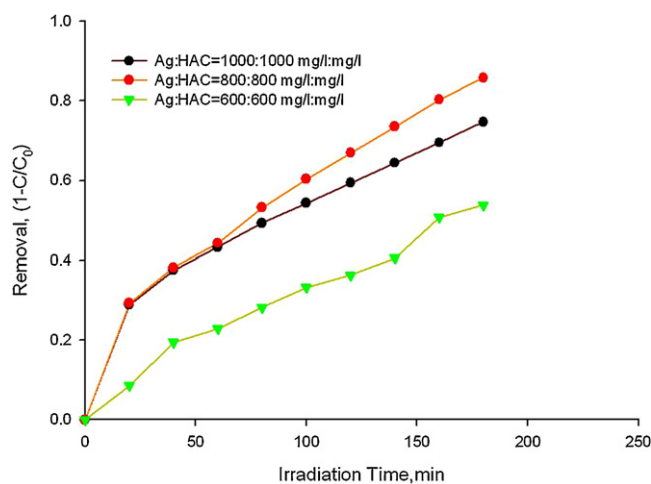


**Fig. 5.** The irradiation time change of silver removal ratio at various silver/acetic acid concentrations (experimental conditions: temperature, 25 °C; experiment volume, 300 ml; circulating rate, 300 ml min<sup>-1</sup>; light intensity, 3 mW cm<sup>-2</sup>).

of 365 nm UV. Instead of recombining with holes, the external circuit allows the photo-generated electrons to jump from valence band (VB) to conduction band (CB) and then transferred to the surface of the graphite cathode where they react with silver ions to make the latter deposited on the cathode surface. The silver reduction reaction is:



Observation of the metal deposition at the graphite cathode surface with XRD (Fig. 3) shows that obvious peaks are observed at  $2\theta$  values of 38.1°, 44.2°, 64.4° and 77.4°. The deposited metal is confirmed to be silver by comparing with the patterns published in Committee on Powder Diffraction Standards (JCPDS) Database (JCPDS No. 04-0783) indicating that using the photo catalytic with an external circuit will be much effective in reducing silver ions into pure silver. Additionally, the binding between the metal deposition and the graphite electrode is not strong; the silver can be easily recovered by scraping or ultrasonic vibrating.

In the photocatalyst or photoelectrical catalyst system, the solution pH is also an important operational parameter to affect metal reduction and organic matter decomposition. Fig. 6 shows the influence of pH on the silver reduction efficiency at 4-h reaction time. When the initial solution pH is 7, silver recovery efficiency is 99.8%; an initial pH of 3 results in 73% silver recovery. This indicates that higher initial solution pH favors the reduction of silver ion.

The zero point of charge ( $\text{pH}_{\text{zpc}}$ ) for  $\text{TiO}_2$  is pH 6. When the solution pH is higher than this level, the  $\text{TiO}_2/\text{Ti}$  thin-film electrode surface is in a negatively charged state that will repulse the photo-generated electrons when the latter are jumping from valence band

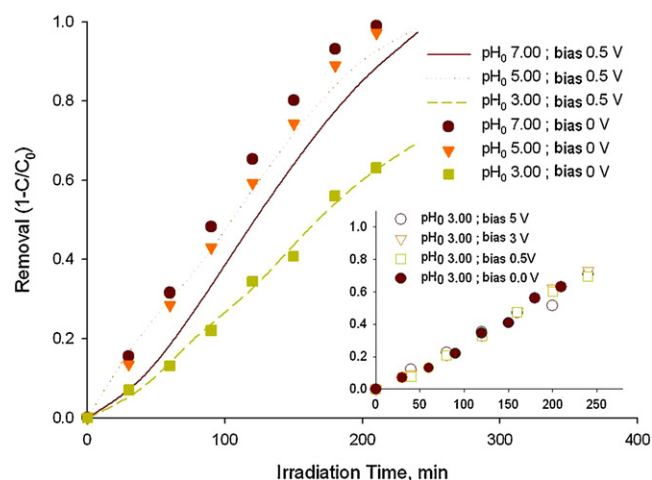


**Fig. 6.** The irradiation time change of silver reduction at various pH and anode bias values (experimental conditions: silver/acetic acid ratio, 108 mg/l:180 mg/l; temperature, 25 °C; circulating rate, 300 ml min<sup>-1</sup>; light intensity, 3 mW cm<sup>-2</sup>).

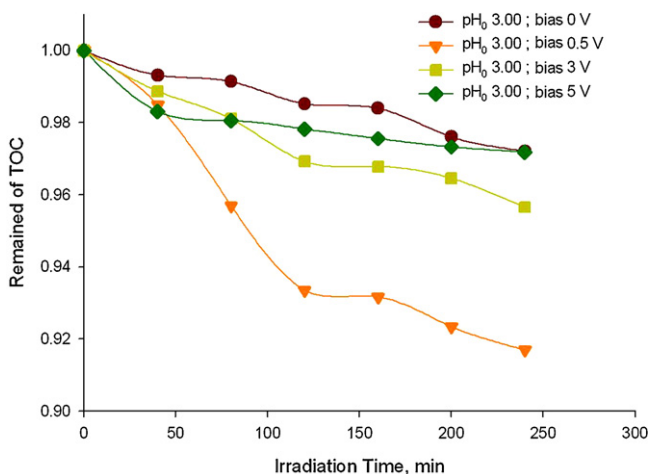


Fig. 7. The irradiation time change of TOC degradation at various anode bias with external circuit (experimental conditions: silver/acetic acid ratio, 108 mg/l:180 mg/l; temperature, 25 °C; circulating rate, 300 ml min<sup>-1</sup>; light intensity, 3 mW cm<sup>-2</sup>).

to conduction band. Using the external electrical circuit will facilitate the transportation of these repulsed electrons to the cathode surface where they may react with silver ions. Additionally, the photo-generated electrons will not be accumulated in the TiO<sub>2</sub>/Ti thin-film electrode thus reducing the probability of electron/hole recombination. The photo-generated holes on the valence band will also be attracted to the surface of TiO<sub>2</sub>/Ti thin-film electrode to raise the production of hydroxyl radicals that enhance the photocatalytic reduction efficiency. Conversely, when the solution pH is lower than TiO<sub>2</sub> p*H*<sub>ZPC</sub>, the TiO<sub>2</sub>/Ti thin-film electrode surface is in a positively charged state that will attract the photo-generated electrons when the latter are jumping from valence band to conduction band. This will allow the silver ions to be reduced at the electrode surface to form silver (Ag<sup>0</sup>). The photo-generated electrons easily accumulated in the TiO<sub>2</sub>/Ti thin-film electrode. With increasing reaction time, the silver deposition will cause a light shielding effect to cause an obvious reduction of the photocatalytic efficiency. Additionally, the photo-generated holes on the valence band are repulsed by the positive charge on the surface of TiO<sub>2</sub>/Ti thin-film electrode and thus cannot be effectively transmitted to the electrode surface. They are accumulated in the TiO<sub>2</sub>/Ti thin-film electrode and recombined with the photo-generated electrons accumulated on the valence band. This results in the reduction of hydroxyl radical generation and photocatalytic decomposition efficiency.

Fig. 6 (inset) shows that if the solution pH is 3, when the anode bias increases from 0, 0.5, 3 to 5 V, the photoelectrical system with external circuit shows no obvious improvement of the silver recovery efficiency, e.g. 73% for 0 V, 70% for 0.5 V, 73% for 3 V and 71% for 5 V. This observation reveals that the photo-generated electrons during the photocatalytic process are passed on to the cathode smoothly without externally applied voltage to cause the electrons to move toward the electrode with similar charges. Fig. 6 also shows that at various pH (3, 5 and 7), that silver recovers efficiency with bias = 0 V is better than that with bias = 0.5 V. It may be inferred that the change pH significantly increase silver recovery efficiency, e.g. 73% for pH 3, 99.2% for pH 5 and 99.8% for pH 7.

Fig. 7 also shows that at pH 3, in 0–5 V range of the anode bias voltage, when the externally applied voltage is 0.5 V, the 240-min light irradiation time will remove 8% TOC. Further increase of the voltage to 5 V will cause the TOC removal efficiency to drop. This is because excessive high externally applied voltage leads to the recombination between the photo-generated holes on the TiO<sub>2</sub> valence band and the electrons formed by the external voltage caus-

ing the efficiency of organic matter mineralization to drop. Hence, providing adequate external voltage is necessary to warranty the passing of photo-generated holes to the electrode surface and raise the efficiency of organic matter decomposition.

#### 4. Conclusions

The APCVD method can be applied to produce nano-level TiO<sub>2</sub> photocatalyst; the APCVD apparatus is easily to set up and is less costly than Direct Current chemical vapor deposition (DCCVD), Micro-wave plasma chemical vapor deposition (MPCVD) or Direct Current magnetron sputtering equipment. Pure water provides oxygen atoms in the TiO<sub>2</sub>/Ti thin-film electrode process thus eliminating the need of pure oxygen and making the process easy to operate. The TiO<sub>2</sub>/Ti thin-film electrode combined with an external circuit and anodic bias is effective in reducing silver ion with 99.8% efficiency. For high-concentrated silver solution (greater than 1000 mg/l Ag), the photocatalytic system will not cause poisoning of TiO<sub>2</sub> electrode and UV shielding thus the TiO<sub>2</sub> photocatalyst activity will not be reduced. When the silver ion concentration is low (108 mg/l Ag), the silver ion concentration in the treated solution meets the effluent limitation for discharge (less than 0.5 mg/l Ag). Although the decomposition of acetic acid in this system is not effective, the residual acetic acid can be removed using other treatment methods. Since the waste photograph fixer solution contains silver, sodium thiosulfate, and acetic acid as the major pollutants, the results published by Huang et al. [11] indicate that the thiosulfate ion ((SO<sub>3</sub><sup>2-</sup>) may behave as scavenger of the photo-generated holes and be oxidized into sulfite (SO<sub>3</sub><sup>2-</sup>) to reduce the recombination of electrons and holes and enhance the photocatalytic efficiency.

#### References

- [1] P.A. Tressure, Silver electrowinning in the EMEW<sup>®</sup> cell, <http://electrowinning.com> (2004) 1–16.
- [2] L.J.J. Janssen, L. Koene, The role of electrochemistry and electrochemical technology in environmental protection, *Chem. Eng. J.* 85 (2002) 137–146.
- [3] F. Fourcade, T. Tzedakis, A. Bergel, Electrochemical process for metal recovery from iodized silver derivatives in liquid/solid mixture: Experimental and theoretical approaches, *Chem. Eng. Sci.* 58 (2003) 3507–3522.
- [4] M. Chatelut, E. Gobert, O. Vittori, Silver electrowinning from photographic fixing solutions using zirconium cathode, *Hydrometallurgy* 54 (2000) 79–90.
- [5] S. Pavlinic, I. Piljac, Electrolytic desorption of silver from ion-exchange resins, *Water Res.* 32 (1998) 2913–2920.
- [6] S. Syed, S. Suresha, L.M. Sharma, A.A. Syed, Clean technology for the recovery of silver from processed radiographic films, *Hydrometallurgy* 63 (2002) 277–280.
- [7] M.O. Adams, On-site gold refining of cyanide liquors by solvent extraction, *Miner. Eng.* 16 (2003) 369–373.
- [8] A.V. Pethkar, K.M. Paknikar, Thiosulfate biodegradation-silver biosorption process for the treatment of photofilm processing wastewater, *Process Biochem.* 38 (2003) 855–860.
- [9] A.I. Zouboulis, Silver recovery from aqueous streams using ion flotation, *Miner. Eng.* 8 (1995) 1477–1488.
- [10] A. Troupis, A. Hiskia, E. Papaconstantinou, Photocatalytic reduction-recovery of silver using polyoxometalates, *Appl. Catal. B: Environ.* 42 (2003) 305–315.
- [11] M. Huang, E. Tso, A.K. Datye, M.R. Prairie, M.B. Stange, Removal of silver in photographic processing waste by TiO<sub>2</sub>-based photocatalysis, *Environ. Sci. Technol.* 30 (1996) 3084–3088.
- [12] T.C. An, X.H. Zhu, Y. Xiong, Feasibility study of photoelectrochemical degradation of methylene blue with three-dimensional electrode-photocatalytic reactor, *Chemosphere* 46 (2002) 897–903.
- [13] T.C. An, Y. Xiong, G.Y. Li, C.H. Zha, X.H. Zhu, Synergetic effect in degradation of formic acid using a new photoelectrochemical reactor, *J. Photochem. Photobiol. A: Chem.* 152 (2002) 155–165.
- [14] C. He, Y. Xiong, X.H. Zhu, A novel method for improving photocatalytic activity of TiO<sub>2</sub> film: the combination of Ag deposition with application of external electric field, *Thin Solid Films* 422 (2002) 235–238.
- [15] E. Szabó-Bárdos, H. Czili, A. Horváth, Photocatalytic oxidation of oxalic acid enhanced by silver deposition on a TiO<sub>2</sub> surface, *J. Photochem. Photobiol. A: Chem.* 154 (2003) 195–201.
- [16] J.A. Byrne, B.R. Eggers, W. Byers, N.M.D. Brown, Photoelectrochemical cell for the combined photocatalytic oxidation of organic pollutants and the recovery of metals from waste waters, *Appl. Catal. B: Environ.* 20 (1999) L85–L89.

- [17] T. Kanki, H. Yoneda, N. Sano, A. Toyoda, C. Nagai, Photocatalytic reduction and deposition of metallic in aqueous phase, *Chem. Eng. J.* 97 (2004) 77–81.
- [18] D. Chen, A.K. Ray, Removal of toxic metal ions from wastewater by semiconductor photocatalysis, *Chem. Eng. Sci.* 56 (2001) 1561–1570.
- [19] Y. Yonezawa, N. Kometani, T. Sakaue, A. Yano, Photo-reduction of silver ions in a colloidal titanium dioxide suspension, *J. Photochem. Photobiol. A: Chem.* 171 (2005) 1–8.
- [20] W.Y. Wang, Y. Ku, Effect of solution pH on the adsorption and photocatalytic reaction behaviors of dyes using TiO<sub>2</sub> and Nafion-coated TiO<sub>2</sub>, *Colloid. Surface. A* 302 (2007) 261–268.
- [21] C.H. Li, Y.H. Hsieh, W.T. Chiu, C.C. Liu, C.L. Kao, Study on preparation and photocatalytic performance of Ag/TiO<sub>2</sub> and Pt/TiO<sub>2</sub> photocatalysts, *Sep. Purif. Technol.* 58 (2007) 148–151.
- [22] L. Kavan, J. Rattouský, M. Grätzel, V. Shklover, A. Zukal, Mesoporous thin film TiO<sub>2</sub> electrodes, *Micropor. Mesopor. Mater.* 44–45 (2001) 653–659.
- [23] R. Palombari, M. Ranchella, C. Rol, G.V. Sebastiani, Oxidative photoelectrochemical technology with Ti/TiO<sub>2</sub> anodes, *Sol. Energy Mater. Sol. C* 71 (2002) 359–368.
- [24] T.C. An, G.Y. Li, X.H. Zhu, J.M. Fu, G.Y. Sheng, Z. Kun, Photoelectrocatalytic degradation of oxalic acid in aqueous phase with a novel three-dimensional electrode-hollow quartz tube photoelectrocatalytic reactor, *Appl. Catal. A: Gen.* 279 (2005) 247–256.
- [25] C. He, X.Z. Li, N. Graham, Y. Wang, Preparation of TiO<sub>2</sub>/ITO and TiO<sub>2</sub>/Ti photoelectrodes by magnetron sputtering for photocatalytic application, *Appl. Catal. A: Gen.* 305 (2006) 54–63.
- [26] A. Hagfeldt, H. Lindström, S. Södergren, S.E. Lindquist, Photoelectrochemical studies of colloidal TiO<sub>2</sub> films: the effect of oxygen studied by photocurrent transients, *J. Electroanal. Chem.* 381 (1995) 39–46.
- [27] M. Radecka, M. Wierzbicka, S. Komornicki, M. Rekas, Influence of Cr on photoelectrochemical properties of TiO<sub>2</sub> thin films, *Phys. B* 348 (2004) 160–168.
- [28] C.C. Yang, M.H. Tsai, Photocatalytic treatment of acetic acid wastewater by nanostructure film of TiO<sub>2</sub>, in: *International Symposium on Environmental Nanotechnology, Proceedings, Taipei, Taiwan, 2004*, pp. 269–274.
- [29] H. Hidaka, H. Nagaok, K. Nohara, T. Shimura, S. Horikoshi, J.C. Zhao, N.C. Serpone, A mechanistic study of the photoelectrochemical oxidation of organic compound on a TiO<sub>2</sub>/TCO particulate film electrode assembly, *J. Photochem. Photobiol. A: Chem.* 98 (1996) 73–78.